Opto-Electronic Advances

ISSN 2096-4579 CN 51-1781/TN

Laser direct writing of Ga_2O_3/liquid metal-based flexible humidity sensors

Songya Cui, Yuyao Lu, Depeng Kong, Huayu Luo, Liang Peng, Geng Yang, Huayong Yang and Kaichen Xu

Citation: Cui SY, Lu YY, Kong DP, Luo HY, Peng L et al. Laser direct writing of Ga_2O_3/liquid metal-based flexible humidity sensors. *Opto-Electron Adv* **6**, 220172(2023).

https://doi.org/10.29026/oea.2023.220172

Received: 27 October 2022; Accepted: 22 February 2023; Published online: 25 April 2023

Opto-Electronic Advances

Article

July 2023, Vol. 6, No. 7

DOI: 10.29026/oea.2023.220172

Laser direct writing of Ga_2O_3/liquid metal-based flexible humidity sensors

Songya Cui[1,2†], Yuyao Lu[1†], Depeng Kong[1], Huayu Luo[1], Liang Peng[2], Geng Yang[1], Huayong Yang[1] and Kaichen Xu[1*]

Flexible and wearable humidity sensors play a vital role in daily point-of-care diagnosis and noncontact human-machine interactions. However, achieving a facile and high-speed fabrication approach to realizing flexible humidity sensors remains a challenge. In this work, a wearable capacitive-type Ga_2O_3/liquid metal-based humidity sensor is demonstrated by a one-step laser direct writing technique. Owing to the photothermal effect of laser, the Ga_2O_3-wrapped liquid metal particles can be selectively sintered and converted from insulative to conductive traces with a resistivity of 0.19 Ω·cm, while the untreated regions serve as active sensing layers in response to moisture changes. Under 95% relative humidity, the humidity sensor displays a highly stable performance along with rapid response and recover time. Utilizing these superior properties, the Ga_2O_3/liquid metal-based humidity sensor is able to monitor human respiration rate, as well as skin moisture of the palm under different physiological states for healthcare monitoring.

Keywords: laser direct writing; liquid metal; humidity sensors; flexible electronics; wearable sensors

Cui SY, Lu YY, Kong DP, Luo HY, Peng L et al. Laser direct writing of Ga_2O_3/liquid metal-based flexible humidity sensors. *Opto-Electron Adv* **6**, 220172 (2023).

Introduction

Recent studies in emerging flexible humidity sensors have achieved great developments in advanced manufacturing methods[1–3], as well as innovative applications including human healthcare detection[4,5], plant health management[6,7] and noncontact human-machine interfaces[8]. Based on different working principles, flexible humidity sensors are mainly categorized into different types including capacitive[4], resistive[9], impedance-type[10], voltage-type[11] and surface acoustic wave[12]. Among them, capacitive-type humidity sensors have gained much attention due to reliable humidity sensing performance, low power consumption and facile structural designs[13,14]. Generally, the performance of a capacitive humidity sensor is strongly correlated with the dielectric permittivity of functional nanomaterials between the electrodes[15]. Until now, various active materials have been investigated as flexible capacitive humidity sensors, such as carbon materials[10,16], cellulose paper[17], metal oxides[18,19], metal sulfides[20,21], and conductive polymer[22]. They are typically endowed with high hydrophilicity, large exposed surface areas and rich active sites to interact with water molecules.

Ga_2O_3, as a potential metal oxide with high chemical and thermal stability, has been employed as an active material for humidity sensors[23,24]. The fabrication techniques to realize Ga_2O_3-based humidity sensors mainly involve chemical vapor deposition (CVD)[25–27], thermal

[1]State Key Laboratory of Fluid Power and Mechatronic Systems, School of Mechanical Engineering, Zhejiang University, Hangzhou 310030, China; [2]School of Information and Electrical Engineering, Hangzhou City University, Hangzhou 310015, China.

†These authors contributed equally to this work.

*Correspondence: KC Xu, E-mail: xukc@zju.edu.cn

Received: 27 October 2022; Accepted: 22 February 2023; Published online: 25 April 2023

treatment[23], and hydrothermal methods[28]. For instance, Tsai et al. proposed a metal-organic CVD growth method to form β-Ga_2O_3 nanowires as sensitive materials in response to humidity changes[25]. Furthermore, the response properties of β-Ga_2O_3-GaS humidity sensors fabricated by thermal treatment at the range from 42% to 92% relative humidity (RH) are presented[23]. Nevertheless, these traditional methods to develop Ga_2O_3-based humidity sensors usually involve high annealing temperature, complicated fabrication procedures as well as various material systems, hindering their practical applications.

Digital laser direct writing is a rapid and environmental-friendly manufacturing approach to generating functional micro/nano-structures or directly creating sensitive nanomaterials with high precision[29–32]. Based on laser-matter interactions, via judiciously selecting the appropriate laser processing parameters, a variety of innovative flexible sensors, such as physical, chemical and physiological sensors have been demonstrated[33–38]. In terms of the flexible humidity sensors by laser processing, the typical strategies usually rely on the laser direct writing of electrodes, followed by the deposition of moisture sensitive nanomaterials, such as carbon or metal sulfides-based materials[6,8,39,40]. However, electrodes and sensitive materials of these humidity sensors are usually fabricated by different processing technologies with multiple procedures. Therefore, a facile manufacturing approach to developing thin film-based humidity sensor is still required.

In this work, a one-step fabrication strategy based on ultraviolet (UV) laser direct writing to realize Ga_2O_3/liquid metal (LM)-based flexible capacitive humidity sensor is proposed. Owing to the centralized heat of UV laser, interdigital electrodes can be rapidly formed with a well-controlled manner through selectively disrupting the superficial Ga_2O_3 layers surrounding the LM particles. This dexterously converts the insulative Ga_2O_3-wrapped LM (GWLM) particles into conductive paths along with the scanning traces of designed patterns. The unsintered regions with Ga_2O_3 layers between electrodes serve as active sensing nanomaterials in response to humidity variations. The resistivity of conductive patterns can be optimized to as low as 0.19 Ω·cm. The humidity sensor presents almost no performance degradation after 46 h measurement. The humidity sensor is applied to monitor the respiration and the sweating during exercise. Hence, this work affords a facile fabrication strategy to realize flexible humidity sensors for healthcare monitoring.

Results and discussion

The fabrication process to realize a flexible Ga_2O_3/LM-based humidity sensor is presented in Fig. 1(a), mainly including ultrasonication, spray-coating and laser sintering. The dispersed solution composed of GWLM particles was obtained by ultrasonication of bulk eutectic gallium-indium (eGaIn) alloy in the ethanol (Fig. 1(a-i)). Then, the dispersed solution was spray-coated on a polyimide (PI) substrate to form a uniform layer of GWLM particles (Fig. 1(a-ii)). This homogeneous layer was non-conductive due to the formation of oxidized layers wrapping each eGaIn particle, resulting in the electrical insulation from each other. Significantly, under the laser treatment, the electrical property can be flexibly tuned by the localized heat of focused UV pulse light, which leads to the thermal expansion of GWLM particles, breaks the oxide shell and then enables the conductive core of LM to leak out. This allows the generation of conductive paths (Fig. 1(a-iii) and 1(b-i, b-ii))[40,41]. Thus, the capacitive humidity sensor was successfully fabricated by this one-step laser processing method. The flexible humidity sensor was composed of two parts, including the uniformly distributed GWLM particles as active sensing materials to the moisture and the conductive electrodes by laser direct writing (Fig. 1(b-i)). Owing to the merits of programmable digital laser patterning, the sizes and configurations of humidity sensors can be dynamically tuned based on controlling laser processing parameters. Here, a typical design of capacitive humidity sensor using interdigital electrodes is employed.

The sensing mechanism of Ga_2O_3/LM-based humidity sensor is similar to the majority of humidity sensors associated with electron transfer processes involving a Grotthuss chain reaction (Fig. 1(b-iii)). At a low RH level, water molecules firstly occupy the hydrophilic sites on the Ga_2O_3 surface to form a chemisorbed layer[23,24]. Then, additional layers of water molecules are superimposed on the first chemisorbed layer through hydrogen bonding at a high RH level[42]. Because of the large accumulation of water molecules on material surfaces, high-density hydroniums are generated under the applied electrostatic field. Subsequently, the proton-hopping occurs among the hydroniums (H_3O^+) and water molecules, which can be described as[8,39,43],

$$H_2O + H_3O^+ = H_3O^+ + H_2O\,. \tag{1}$$

The proton hopping based on the Grotthuss mechanism is responsible for changing the capacitance of

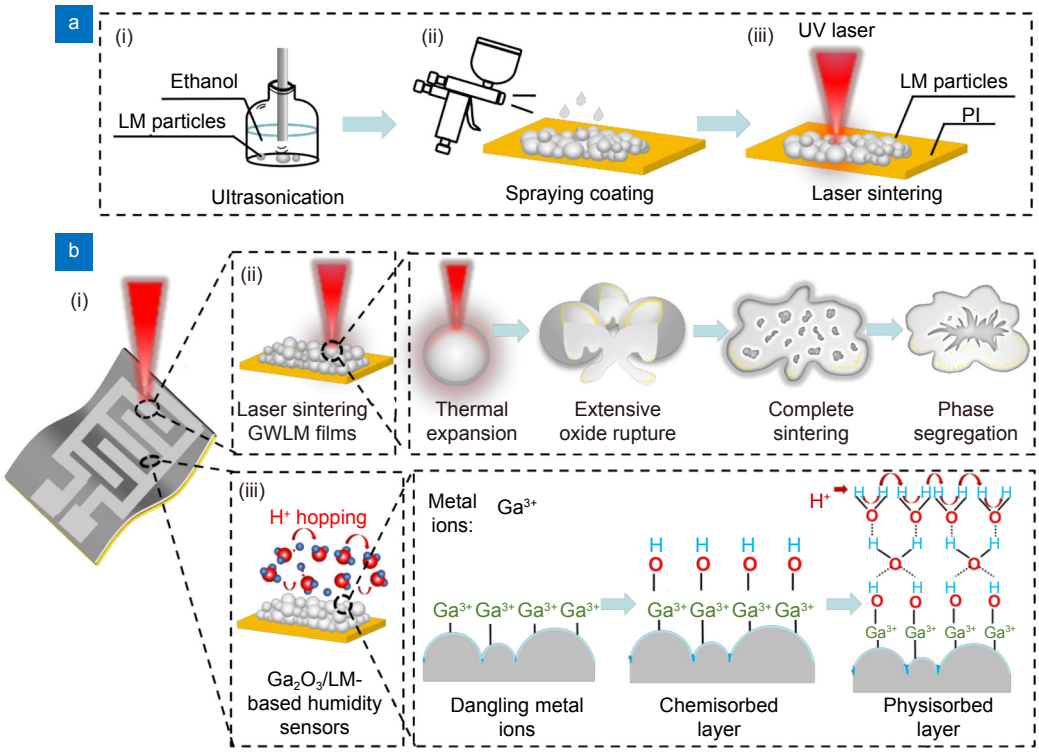

Fig. 1 | Design and fabrication of flexible capacitive humidity sensors. (**a**) Fabrication processes of flexible Ga_2O_3/LM humidity sensors, including ultrasonication, spraying coating and laser sintering. (**b**) Schematic of the mechanism to form GWLM films by laser sintering and the sensing mechanism of Ga_2O_3/LM-based humidity sensors.

Ga_2O_3/LM-based humidity sensor. The capacitance (C_{sensor}) can be defined as[44],

$$C_{sensor}=\frac{\varepsilon_e S}{4\pi k d}, \tag{2}$$

where ε_e is dielectric permittivity, S is electrode area, k is electrostatic force constant, d is the distance of parallel plate. In Eq. (2), the C_{sensor} is proportional to ε_e when S and d are constant values. The dielectric constant of Ga_2O_3 is about 10.0, while pure water has a lager value of around 78.5[45,46]. With increasing the RH, the water molecules tend to penetrate into the humidity sensitive layers of GWLM, leading to the increase of capacitance due to the high permittivity of moisture.

Based on the aforementioned principles, this Ga_2O_3/LM-based flexible humidity sensor was fabricated by a pulsed UV laser. To clearly show the surface morphologies of GWLM particles and conductive patterns after laser treatment, scanning electron microscope (SEM) images of corresponding samples were characterized (Fig. 2(a–e)). As observed in Fig. 2(a–e), a fully interconnected liquid metal network was formed, indicating that thermal stress generated by the photothermal effect of the laser beam was sufficient to cause extensive rupture of the oxide skin of the particles, allowing liquid cores to flow out and merge into wrinkled continuous structures[41]. This implies the formation of conductive paths (Fig. 2(b–d)). To figure out the elemental composition of the sensing materials, the energy-dispersive X-ray spectroscopy (EDX) was also performed (Fig. 2(f)). The elemental mapping results indicated the homogeneous distribution of each element including Ga, In and O in the material system. The ultrasonication and spray-coating of eGaIn on PI film allowed the formation of nonconductive networks with the diameter of most GWLM particles at around 300 nm (Fig. 2(g)). It was found that at a relatively low laser fluence (2.8 J/cm^2), only a few GWLM particles on the surface were sintered into conductive patterns with a resistivity of ~10^5 Ω·cm (Fig. 2(h)). Increasing the laser fluence resulted in the combination of more GWLM particles and then lower resistivity. When the intensity of laser fluence is over 6.8 J/cm^2, a much lower resistivity at around 0.19 Ω·cm can be achieved. Figure 2(i) shows a conductive LM path with a line width of 48.3 μm. Thus, such a digital laser processing strategy affords to not only pattern LM-based electrodes, but also flexibly tune the conductivity of electrodes. In addition, wettability analysis of this sensor was evaluated by measuring static

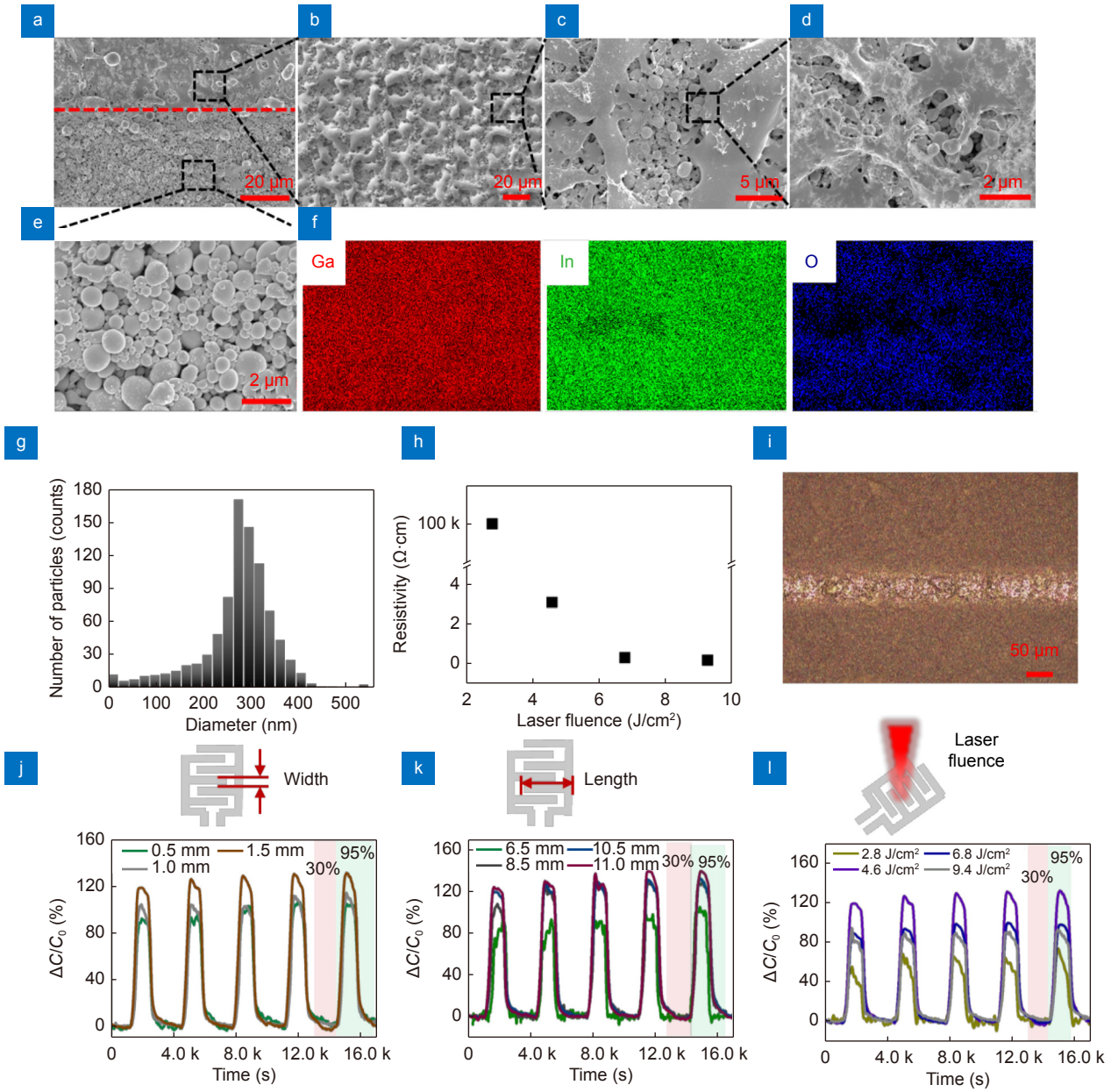

Fig. 2 | Characterizations of flexible humidity sensors. SEM images of GWLM (**a**–**d**) with and (a, **e**) without laser sintering. (**f**) EDX images of the Ga, In, and O distributions. (**g**) Histogram of diameter size distribution for the unsintered GWLM particles on the PI film. (**h**) Resistivity of the laser induced conductive GWLM paths at different laser fluences. (**i**) The minimum resolution of sintered LM path at a laser fluence of 9.4 J/cm². (**j**–**l**) Schematics of Ga_2O_3/LM-based humidity sensors with various fabrication parameters (i.e. widths and lengths of electrodes, UV laser fluence) (top). Cycle measurements of Ga_2O_3/LM-based humidity sensors by periodically varying the humidity from 30% RH to 95% RH (bottom).

contact angles. The water contact angle for unsintered GWLM films was 65° (Fig. S1(a)). In contrast, the contact angle decreases to 19° after sintering GWLM films (Fig. S1(b)). This superior hydrophilic property provides an ideal functional surface to attract water molecules for humidity sensing applications.

To study the humidity effect on the performance of this humidity sensor, the capacitance values were characterized in an oven with controllable temperature and humidity. The humidity sensors with varying interdigital electrodes and laser processing parameters were realized by the one-step laser sintering procedure. During the measurements, the temperature was controlled at a constant value (20 °C). Initially, the cycle tests of Ga_2O_3/LM-based humidity sensors with various widths (W) of electrodes were conducted at a humidity range from 30% RH to 95% RH (Fig. 2(j)). It is obvious that the humidity performance shows an increasing trend as the width of

electrodes increases. When the width of electrodes is 1.5 mm, the Ga_2O_3/LM-based humidity sensor exhibits the highest capacitance change of 136.3%. This is probably attributed to the enhanced charge transfer when the gap of adjacent electrodes becomes small (Fig. S2(a, b))[42]. Meanwhile, the performances of humidity sensors with different lengths (L) of finger electrodes were investigated (Fig. 2(k)). The Ga_2O_3/LM-based humidity sensor displays the highest capacitance change of up to 142.4% with electrodes length of 11 mm. According to the Eq. (2), the sensing area between active layers and electrodes becomes larger with the longer electrodes, leading to the enhancement of capacitance (Fig. S2(c))[47]. To figure out the relationship between humidity performances and laser fluences, the cyclic performance of Ga_2O_3/LM humidity sensor processed with different laser powers was performed (Fig. 2(l)). It is illustrated that the humidity sensor fabricated at a 4.6 J/cm^2 laser fluence presents the highest capacitance change of 136.3%. This is due to that at the weaker laser fluence (<4.6 J/cm^2), only GWLM particles on the shallow surface were sintered to form the electrode paths (Fig. S2(d)). In addition, at the larger laser fluence (>4.6 J/cm^2), the thickness of sintered electrodes become smaller due to the ablation effect. Both cases resulted in the reduction of sensing area between the electrodes and effective functional layer. Therefore, to obtain a humidity sensor with optimal performance, it is significant to select the appropriate parameters including widths and lengths of electrodes, as well as the laser fluence[48,49].

In order to compare the performance of humidity devices fabricated by various laser wavelengths, the humidity response of Ga_2O_3/LM sensor sintered by a CO_2 laser was also investigated. The humidity response of the device sintered by the CO_2 laser in Fig. S3 shows relatively poor performance with 47% capacitance change when the RH varied from 30% to 95%. A 355 nm pulsed laser may be a better candidate for laser processing due to that it has relatively smaller thermal effect than CO_2 laser, thus slowing the speed of re-oxidation of the sintered LM electrodes[50]. Therefore, the humidity sensors fabricated by the UV laser are more reliable due to their relatively high sensitivity and reproducibility.

Based on the aforementioned fundamental characterizations, a Ga_2O_3/LM humidity sensor with an electrode width of 1.5 mm and length of 11 mm was created at a laser fluence of 4.6 J/cm^2 for further investigations. A photo of the Ga_2O_3/LM flexible humidity sensor composed of laser-sintered interdigital electrodes (light grey) and untreated sensing materials (dark grey) is presented in Fig. 3(a). To clearly show the sensitivity of this humidity sensor at different RHs, the capacitance changes of Ga_2O_3/LM humidity sensors were tested from 30% RH to 95% RH. Although the capacitance changes of the humidity sensors present a nonlinear characteristic, the capacitance changes are still clearly captured at a wide variety of RHs. When the RH increases from 30% RH to 95% RH, the humidity sensor displays a capacitance change of ~102.2% (Fig. 3(b)). For the majority of humidity sensors, temperature usually has interference on the output of humidity sensor. To evaluate this cross-talk issue, the capacitance changes of a humidity sensor covered by a piece of gas-proof PET membrane were measured at varied temperatures from 25 °C to 45 °C. The real-time temperatures were monitored by a commercial temperature sensor. Via periodically changing the oven temperature, the Ga_2O_3/LM humidity sensor displays slight fluctuation of capacitance change within 4% (Fig. 3(c)).

Next, to apply the LM-based humidity sensor in practical applications, signal reproducibility is of high importance. Here, 50 cycles' measurement between 30% and 95% RH was conducted (Fig. 3(d, e)). A highly stable cycling behavior was observed at 95% RH for more than 46 h with almost no performance degradation. In addition, four samples with electrodes width of 0.5 mm and length of 11 mm were fabricated by UV laser fluence of 4.6 J/cm^2. To investigate batch-to-batch reproducibility, cycle measurements of these four different humidity sensors by periodically varying the humidity from 30% RH to 95% RH were tested (Fig. 3(f)). Furthermore, to validate the mechanical bending effect on the humidity sensor, a real-time bending test for the Ga_2O_3/LM-based humidity sensor was performed (Fig. S4). The relatively small variations (<7.4%) under diverse bending radii are probably attributed to the change of the electrode distance and sensing area of humidity sensor induced by the device deformation.

Using the proposed flexible humidity sensors, two important applications were performed. Human breathing monitoring has gained much attention as one of the vital signals for health management. To conduct this, a humidity sensor was attached to a commercial mask on an adult's face (Fig. 4(a)). The humidity response of respiration demonstrates a high repeatability in five measurement periods (Fig. 4(b)). Due to the high moisture induced by the breath, the capacitance change of

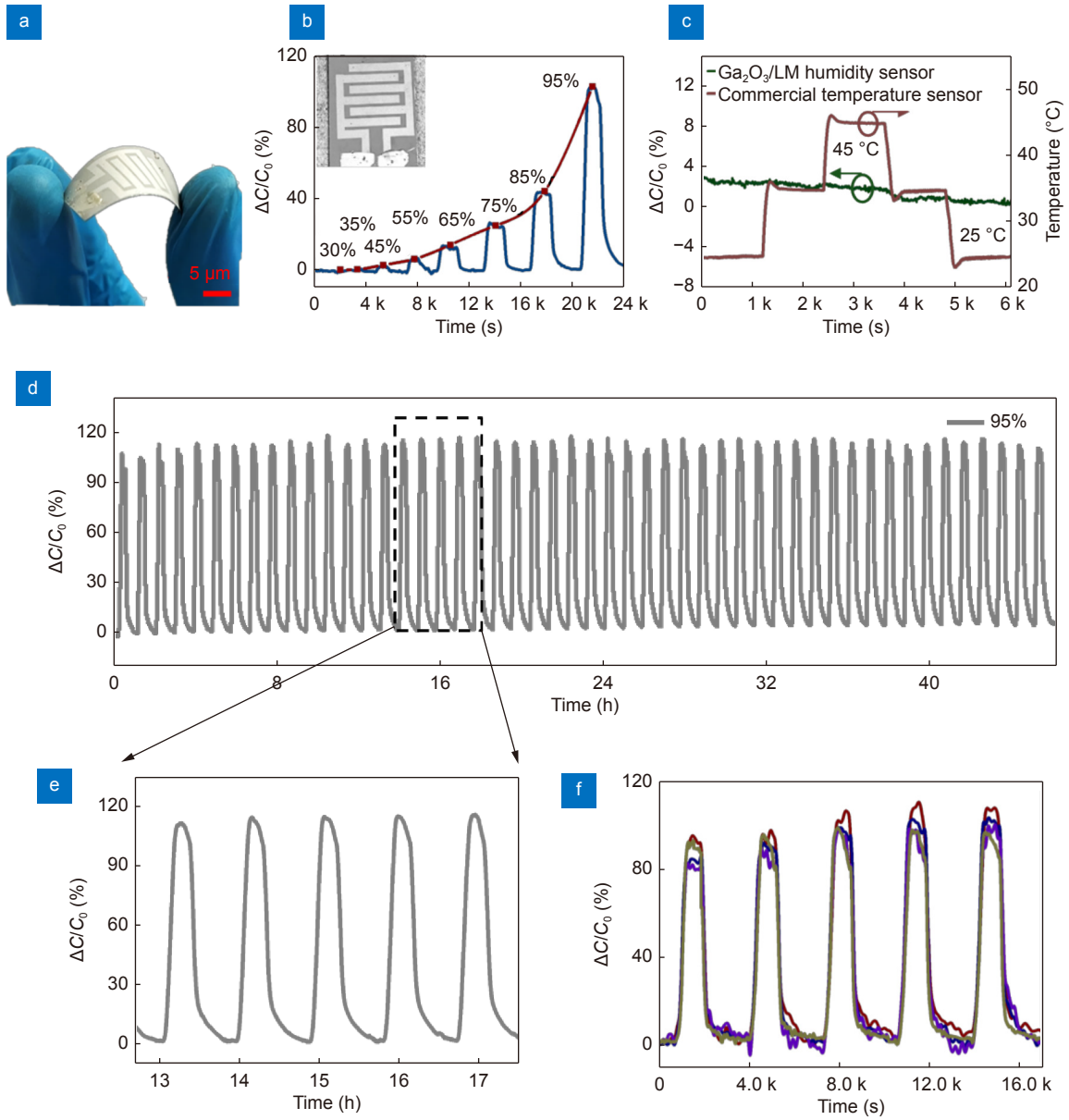

Fig. 3 | (**a**) Photo of a flexible Ga_2O_3/LM-based humidity sensor. (**b**) Capacitance change of Ga_2O_3/LM-based humidity sensor at different RHs. The inset shows the image of this sensor. (**c**) A temperature dependent test of Ga_2O_3/LM-based humidity sensor via varying temperatures from 25 °C to 45 °C. The temperature in the oven was recorded by a commercial thermal sensor. (**d, e**) Long-term stability measurement (50 cycles) under 95% RH. (**f**) Cycle measurements of four different batches of humidity sensors by periodically varying the humidity from 30% RH to 95% RH.

193.1% was observed for the respiration monitoring. Furthermore, the humidity performance of long-time breathing monitoring by nose confirms the high sensitivity and fast response of the Ga_2O_3/LM-based humidity sensors (Fig. 4(c–f)). The response and recovery time as two vital humidity parameters to evaluate the response speeds of a humidity device. Notably, this capacitive humidity sensor displays a very fast response time (t_1~1.2 s) according to the respiration test (Fig. 4(c)). This rapid response is probably attributed to enormous numbers of hydrophilic groups inside the Ga_2O_3 particle systems. It is known that the oxides have high possibility to form hydrogen bonds with the chemically or physically absorbed water molecules. Such feature provides the Ga_2O_3 nanoparticles with a superior hydrophilic property. The sensing material that is endowed with this property usually presents high sensitivity and fast response due to the effective transfer of protons on the surface occupied by multiple water molecules. Additionally, it took about 1.6 s (t_2) for the device to recover to its original dry condition, indicating that the desorption of water molecules is also fast. These results are comparable to other

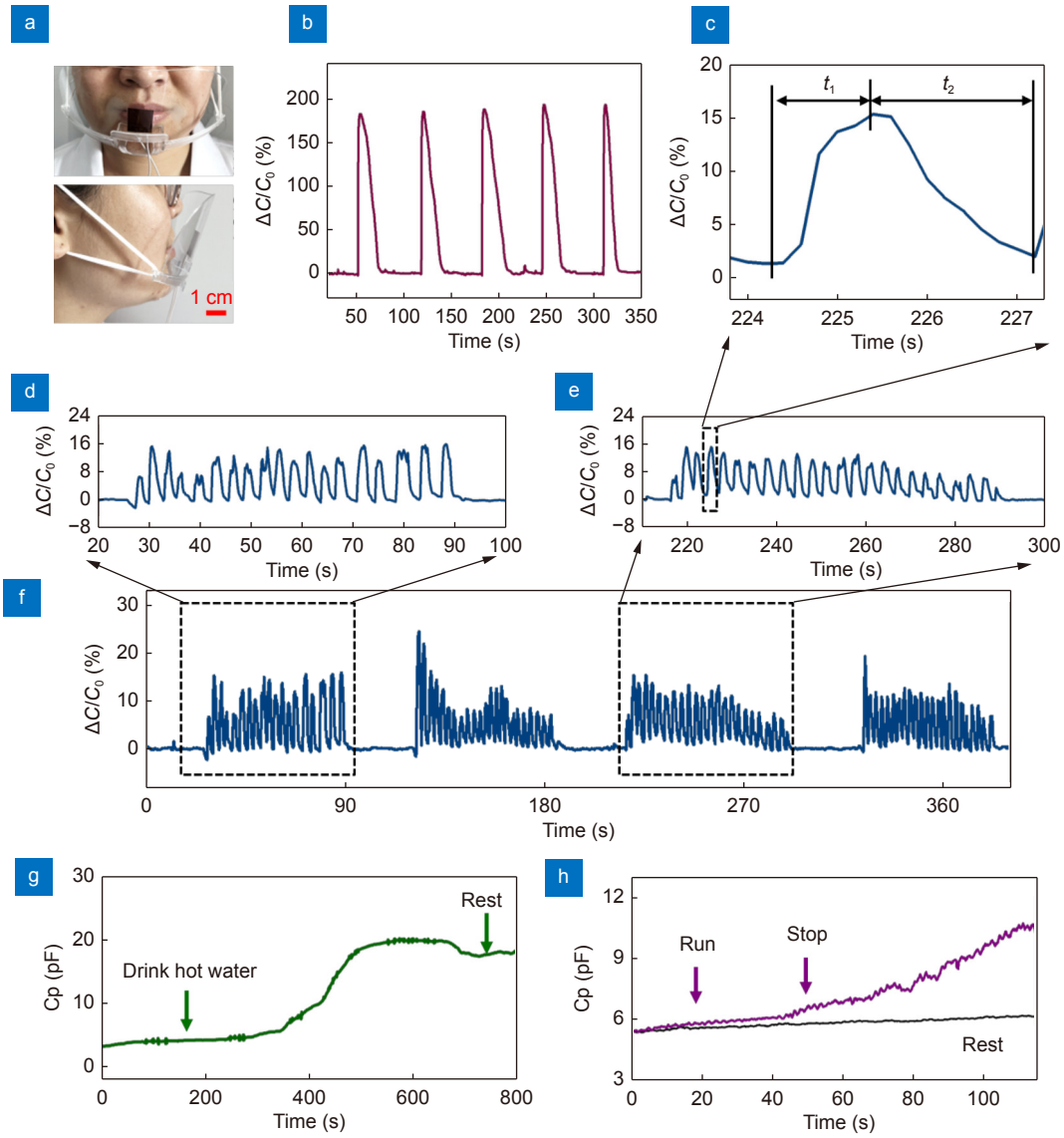

Fig. 4 | (**a**) Photos of a humidity sensor on a commercial mask worn on the subject's face. (**b**) Human respiration test of a subject by mouth at a rest state. (**c**) Response and recovery time of the sensor. (**d–f**) Real-time monitoring of respiratory rate by nose of a subject at a rest state. Real-time monitoring of palm moisture while (**g**) drinking hot water and (**h**) exercising.

thin film-based humidity sensors (Table S1). In addition, the measured breathing rate of this subject was about 18 times/min, which agreed with the respiratory rate (12–20 times/min) of a healthy adult (Fig. 4(d–f))[51].

Another significant application is to detect the sweat evaporation from human skin while drinking hot water and exercising. By attaching the humidity device on the palm of a hand, the moisture condition can be captured during drinking hot water. Generally, the temperature of human body is regulated by heat loss from pores, which is usually accompanied by sweating[52]. A healthy adult usually regulates body temperature by sweating after physical activities. The image of this sensor attached on the hand palm is displayed in Fig. S5. Here, the real-time humidity variation of a palm during drinking hot water was performed (Fig. 4(g)). At the beginning, the capacitance maintained a stable value at around 3.3 pF. After drinking 150 mL hot water, the capacitance gradually increased. The capacitance change is about 16.7 pF after about 325 s of drinking water and keeps the C_{sensor} at ~20.0 pF for around 160 s. This implies that the skin tends to balance the water content in the body and releases the moisture when necessary to decrease the body temperature. After some time, the capacitance of humidity sensor slightly decreased to 18.2 pF, indicating that the body state gradually recovered[39]. Additionally, the real-time palm moisture under exercising was also monitored (Fig. 4(h)). The water loss process of this adult was

captured at two different physical states (exercising and rest states). At the rest state, the capacitance of humidity sensor shows a relatively stable value (~5.5 pF). Upon running, the capacitance output of humidity sensor gradually increased from 5.4 pF to 10.5 pF, indicating a high moisture level on the palm skin. Even the volunteer stopped running, the capacitance continued increasing, implying the slow recovery of body temperature. In summary, the Ga_2O_3/LM-based humidity sensor can serve as a potential device for real-time healthcare monitoring.

Conclusions

In summary, the Ga_2O_3/LM-based flexible humidity sensors realized by one-step UV laser direct writing approach are studied. The photothermal effect of laser irradiation results in the combination of insulative Ga_2O_3/LM particles, leading to the high conductivity of interdigital electrodes, while the untreated regions are applied as active sensing materials in response to moisture variations. It is found that this humidity sensor presents long-term stability (46 h measurement) with a rapid response (~1.2 s) and recovery time (~1.6 s). This one-step digital laser direct writing approach paves a new way to fabricate flexible and wearable humidity sensors for practical applications towards human health monitoring.

Experimental section

Fabrication of Ga_2O_3/LM-based flexible humidity sensors

The GWLM dispersion was made by mixing eGaIn (75% Ga, 25% In, 200 mg) with ethanol (10 mL), followed by the sonication with a sonicator probe (Dowell, DW-SD28-300B) for 30 min. The solution was simultaneously cooled in an ice-water bath. Prior to spraying, a vortex mixer was applied for vigorous mixing to ensure uniform GWLM dispersion. To obtain uniform GWLM particles on the thin film, a spray equipment was employed consisting of a spray gun (Anest Iwata, W-101) and an air pump (30 L). The GWLM dispersion was sprayed onto the surface of a PI film to form uniform GWLM particle layers, which were naturally dried in the air. To create conductive paths, the GWLM particles were selectively sintered by a nanosecond UV laser (FOTIA-355–5–30-W, Advanced Optowave, USA) with a wavelength of 355 nm and pulse repetition rate of 20 kHz. The laser fluence was varied from 2.8 to 9.4 J/cm^2, while the scanning speed was fixed at 500 mm/s. In addition, a CO_2 laser (Universal Laser Systems VLS3.50) with a 10.6 μm wavelength was selected as a comparison.

Characterizations of Ga_2O_3/LM-based flexible humidity sensors

Surface morphology of the sensor was characterized by a thermal field emission scanning electron microscope (SEM, Hitachi SU-70 UHR), which was equipped with an energy dispersive X-ray (EDX) detector for the elemental analysis. Resistance measurements of the Ga_2O_3/LM humidity sensors were performed by a digital multimeter (Keysight, 34470A). The relative humidity and temperature responses of the sensor were dynamically measured in a bench-top environment oven (Espec, SH-262). Commercial temperature and humidity sensors were applied to calibrate the temperature and humidity in the oven. The capacitance was measured using an LCR multimeter (Keysight, E4980AL) with a measurement frequency of 100 kHz. The bending tests were conducted by attaching the device onto the curved surfaces with different radii.

References

1. Kim J, Lee M, Shim HJ, Ghaffari R, Cho HR et al. Stretchable silicon nanoribbon electronics for skin prosthesis. *Nat Commun* **5**, 5747 (2014).
2. Naqi M, Lee S, Kwon HJ, Lee MG, Kim M et al. A fully integrated flexible heterogeneous temperature and humidity sensor - based occupancy detection device for smart office applications. *Adv Mater Technol* **4**, 1900619 (2019).
3. Zhang J Q, Gao Y, Li C et al. Laser direct writing of flexible antenna sensor for strain and humidity sensing. *Opto-Electron Eng* **49**, 210316 (2022).
4. Shen YK, Hou SJ, Hao DD, Zhang X, Lu Y et al. Food-based highly sensitive capacitive humidity sensors by inkjet printing for human body monitoring. *ACS Appl Electron Mater* **3**, 4081–4090 (2021).
5. Guo HY, Lan CY, Zhou ZF, Sun PH, Wei DP et al. Transparent, flexible, and stretchable WS_2 based humidity sensors for electronic skin. *Nanoscale* **9**, 6246–6253 (2017).
6. Lan LY, Le XH, Dong HY, Xie J, Ying YB et al. One-step and large-scale fabrication of flexible and wearable humidity sensor based on laser-induced graphene for real-time tracking of plant transpiration at bio-interface. *Biosens Bioelectron* **165**, 112360 (2020).
7. Lu YY, Xu KC, Zhang LS, Deguchi M, Shishido H et al. Multimodal plant healthcare flexible sensor system. *ACS Nano* **14**, 10966–10975 (2020).
8. Lu YY, Yang G, Shen YJ, Yang HY, Xu KC. Multifunctional flexible humidity sensor systems towards noncontact wearable electronics. *Nanomicro Lett* **14**, 150 (2022).
9. Kano S, Kim K, Fujii M. Fast-response and flexible nanocrystal-based humidity sensor for monitoring human respiration and

water evaporation on skin. *ACS Sens* **2**, 828–833 (2017).
10. Peng XY, Chu J, Aldalbahi A, Rivera M, Wang LD et al. A flexible humidity sensor based on KC–MWCNTs composites. *Appl Surf Sci* **387**, 149–154 (2016).
11. Gu L, Zhou D, Cao JC. Piezoelectric active humidity sensors based on lead-free $NaNbO_3$ piezoelectric nanofibers. *Sensors* **16**, 833 (2016).
12. Wu JH, Yin CS, Zhou J, Li HL, Liu Y et al. Ultrathin glass-based flexible, transparent, and ultrasensitive surface acoustic wave humidity sensor with ZnO nanowires and graphene quantum dots. *ACS Appl Mater Interfaces* **12**, 39817–39825 (2020).
13. Najeeb MA, Ahmad Z, Shakoor RA. Organic thin-film capacitive and resistive humidity sensors: a focus review. *Adv Mater Interfaces* **5**, 1800969 (2018).
14. Kim J, Cho JH, Lee HM, Hong SM. Capacitive humidity sensor based on carbon black/polyimide composites. *Sensors* **21**, 1974 (2021).
15. Duan ZH, Jiang YD, Tai HL. Recent advances in humidity sensors for human body related humidity detection. *J Mater Chem C* **9**, 14963–14980 (2021).
16. Zhu CC, Tao LQ, Wang Y, Zheng K, Yu JB et al. Graphene oxide humidity sensor with laser-induced graphene porous electrodes. *Sens Actuators B Chem* **325**, 128790 (2020).
17. Guan X, Hou ZN, Wu K, Zhao HR, Liu S et al. Flexible humidity sensor based on modified cellulose paper. *Sens Actuators B Chem* **339**, 129879 (2021).
18. Sriphan S, Charoonsuk T, Khaisaat S, Sawanakarn O, Pharino U et al. Flexible capacitive sensor based on 2D-titanium dioxide nanosheets/bacterial cellulose composite film. *Nanotechnology* **32**, 155502 (2021).
19. Velumani M, Meher SR, Alex ZC. Composite metal oxide thin film based impedometric humidity sensors. *Sens Actuators B Chem* **301**, 127084 (2019).
20. Tang HY, Sacco LN, Vollebregt S, Ye HY, Fan XJ et al. Recent advances in 2D/nanostructured metal sulfide-based gas sensors: mechanisms, applications, and perspectives. *J Mater Chem A* **8**, 24943–24976 (2020).
21. Ren J, Guo BJ, Feng Y, Yu K. Few-layer MoS_2 dendrites as a highly active humidity sensor. *Phys E:Low-Dimens Syst Nanostructures* **116**, 113782 (2020).
22. Eryürek M, Tasdemir Z, Karadag Y, Anand S, Kilinc N et al. Integrated humidity sensor based on SU-8 polymer microdisk microresonator. *Sens Actuators B Chem* **242**, 1115–1120 (2017).
23. Sprincean V, Caraman M, Spataru T, Fernandez F, Paladi F. Influence of the air humidity on the electrical conductivity of the β-Ga_2O_3-GaS structure: air humidity sensor. *Appl Phys A* **128**, 303 (2022).
24. Wang D, Lou YL, Wang R, Wang PP, Zheng XJ et al. Humidity sensor based on Ga_2O_3 nanorods doped with Na^+ and K^+ from GaN powder. *Ceram Int* **41**, 14790–14797 (2015).
25. Tsai TY, Chang SJ, Weng WY, Liu S, Hsu CL et al. β−Ga_2O_3 nanowires-based humidity sensors prepared on GaN/sapphire substrate. *IEEE Sens J* **13**, 4891–4896 (2013).
26. Juan YM, Chang SJ, Hsueh HT, Wang SH, Weng WY et al. Effects of humidity and ultraviolet characteristics on β-Ga_2O_3 nanowire sensor. *RSC Adv* **5**, 84776–84781 (2015).
27. Domènech-Gil G, Peiró I, López-Aymerich E, Moreno M, Pellegrino P et al. Room temperature humidity sensor based on single β-Ga_2O_3 nanowires. *Proceedings* **2**, 958 (2018).
28. Pilliadugula R, Gopalakrishnan N. Room temperature ammonia sensing performances of pure and Sn doped β-Ga_2O_3. *Mater Sci Semicond Process* **135**, 106086 (2021).
29. Xu KC, Fujita Y, Lu YY, Honda S, Shiomi M et al. A wearable body condition sensor system with wireless feedback alarm functions. *Adv Mater* **33**, 2008701 (2021).
30. Zhang CJ, Li ZK, Li HY, Yang Q, Wang H et al. Femtosecond laser-induced supermetalphobicity for design and fabrication of flexible tactile electronic skin sensor. *ACS Appl Mater Interfaces* **14**, 38328–38338 (2022).
31. Son Y, Yeo J, Moon H, Lim TW, Hong S et al. Nanoscale electronics: digital fabrication by direct femtosecond laser processing of metal nanoparticles. *Adv Mater* **23**, 3176–3181 (2011).
32. Wolf A, Dostovalov A, Bronnikov K, Skvortsov M, Wabnitz S et al. Advances in femtosecond laser direct writing of fiber Bragg gratings in multicore fibers: technology, sensor and laser applications. *Opto-Electron Adv* **5**, 210055 (2022).
33. Luo HY, Lu YY, Xu YH, Yang G, Cui SY et al. A fully soft, self-powered vibration sensor by laser direct writing. *Nano Energy* **103**, 107803 (2022).
34. Hepp M, Wang HZ, Derr K, Delacroix S, Ronneberger S et al. Trained laser-patterned carbon as high-performance mechanical sensors. *npj Flex Electron* **6**, 3 (2022).
35. Rodriguez RD, Shchadenko S, Murastov G, Lipovka A, Fatkullin M et al. Ultra‐robust flexible electronics by laser‐driven polymer‐nanomaterials integration. *Adv Funct Mater* **31**, 2008818 (2021).
36. Shin J, Jeong B, Kim J, Nam VB, Yoon Y et al. Sensitive wearable temperature sensor with seamless monolithic integration. *Adv Mater* **32**, 1905527 (2020).
37. Zhang CY, Zhou W, Geng D, Bai C, Li WD et al. Laser direct writing and characterizations of flexible piezoresistive sensors with microstructures. *Opto-Electron Adv* **4**, 200061 (2021).
38. Liao J N, Zhang D S, Li Z G. Advance in femtosecond laser fabrication of flexible electronics. *Opto-Electron Eng* **49**, 210388 (2022).
39. Lu YY, Xu KC, Yang MQ, Tang SY, Yang TY et al. Highly stable Pd/HNb_3O_8-based flexible humidity sensor for perdurable wireless wearable applications. *Nanoscale Horiz* **6**, 260–270 (2021).
40. Liu SL, Yuen MC, White EL, Boley JW, Deng B et al. Laser sintering of liquid metal nanoparticles for scalable manufacturing of soft and flexible electronics. *ACS Appl Mater Interfaces* **10**, 28232–28241 (2018).
41. Liu SL, Reed SN, Higgins MJ, Titus MS, Kramer-Bottiglio R. Oxide rupture-induced conductivity in liquid metal nanoparticles by laser and thermal sintering. *Nanoscale* **11**, 17615–17629 (2019).
42. Mahapatra PL, Das S, Mondal PP, Das T, Saha D et al. Microporous copper chromite thick film based novel and ultrasensitive capacitive humidity sensor. *J Alloys Compd* **859**, 157778 (2021).
43. Zhang JJ, Sun L, Chen C, Liu M, Dong W et al. High performance humidity sensor based on metal organic framework MIL-101(Cr) nanoparticles. *J Alloys Compd* **695**, 520–525 (2017).
44. Ma LY, Wu RH, Patil A, Zhu SH, Meng ZH et al. Full‐textile wireless flexible humidity sensor for human physiological monitoring. *Adv Funct Mater* **29**, 1904549 (2019).
45. Passlack M, Schubert EF, Hobson WS, Hong M, Moriya N et al. Ga_2O_3 films for electronic and optoelectronic applications. *J Appl Phys* **77**, 686–693 (1995).

46. Oshima T, Kaminaga K, Mukai A, Sasaki K, Masui T et al. Formation of semi-insulating layers on semiconducting β-Ga_2O_3 single crystals by thermal oxidation. *J Appl Phys* **52**, 051101 (2013).
47. He J, Zheng XT, Zheng ZW, Kong DG, Ding K et al. Pair directed silver nano-lines by single-particle assembly in nanofibers for non-contact humidity sensors. *Nano Energy* **92**, 106748 (2022).
48. Hu GQ, Guan K, Lu LB, Zhang JR, Lu N et al. Engineered functional surfaces by laser microprocessing for biomedical applications. *Engineering* **4**, 822–830 (2018).
49. Yu YC, Bai S, Wang ST, Hu AM. Ultra-short pulsed laser manufacturing and surface processing of microdevices. *Engineering* **4**, 779–786 (2018).
50. Liu SLZ, Kim SY, Henry KE, Shah DS, Kramer-Bottiglio R. Printed and laser-activated liquid metal-elastomer conductors enabled by ethanol/PDMS/liquid metal double emulsions. *ACS Appl Mater Interfaces* **13**, 28729–28736 (2021).
51. Liu XH, Zhang DZ, Wang DY, Li TT, Song XS et al. A humidity sensing and respiratory monitoring system constructed from quartz crystal microbalance sensors based on a chitosan/polypyrrole composite film. *J Mater Chem A* **9**, 14524–14533 (2021).
52. Heng WZ, Yang G, Kim WS, Xu KC. Emerging wearable flexible sensors for sweat analysis. *Biodes Manuf* **5**, 64–84 (2022).

Acknowledgements

This study was supported by the National Natural Science Foundation of China (52105593 and 62271439), STI 2030 —Major Projects (2022ZD0208601) and the “Pioneer” and “Leading Goose” R&D Program of Zhejiang (2023C01051).

Competing interests

The authors declare no competing financial interests.

Supplementary information

Supplementary information is available for this paper at https://doi.org/10.29026/oea.2023.220172